Advanced Materials 28 (2016): 2421 - 2426

DOI: http://dx.doi.org/10486/10.1002/adma.201505020

Thermal Scanning at Cellular Level by an Optically Trapped Upconverting Fluorescent Particle

*Paloma Rodríguez-Sevilla, Yuhai Zhang, Patricia Haro-González, Francisco Sanz-Rodríguez, Francisco Jaque, José García Solé, Xiaogang Liu and Daniel Jaque**

Paloma Rodríguez-Sevilla, Dr. Patricia Haro-González, Dr. Francisco Sanz-Rodríguez, Prof. Francisco Jaque, Prof. José García Sole, and Dr. Daniel Jaque*
Fluorescence Imaging Group, Departamento de Física de Materiales, Facultad de Ciencias, Universidad Autonoma de Madrid, Madrid 28049, Spain
E-mail: daniel.jaque@uam.es

Yuhai Zhang and Xiaogang Liu
Department of Chemistry, National University of Singapure, 3 Science Drive 3, Singapore 117543, Singapore

Keywords: optical trapping, luminescence nanothermometry, plasmonic *in vitro* heating

ABSTRACT

Single particle spectroscopy in the form of three-dimensional optical manipulation of an upconverting nanoparticle is here used for non-invasive thermal sensing at the cellular level. In particular, a single infrared 980 nm laser beam is used as a three-dimensional optical tweezer and, simultaneously, as an optical excitation source for a single $NaYF_4$:Er^{3+},Yb^{3+} upconverting particle. Real time analysis of the thermosensitive green emission of Er^{3+} ions obtained after Yb^{3+} excitation provides thermal sensing during optical manipulation. Thus, three-dimensional particle scanning allows for the measurement of thermal gradients in the surroundings of individual cancer cells subjected to a plasmonic-mediated photothermal therapy. It is found that such thermal gradients extends for distances larger than 10 microns, avoiding real single cell photothermal treatments under *in vitro* conditions. This work introduces to the scientific community a novel and simple approach for high resolution thermal sensing at the cellular level that could constitute a powerful tool for a better understanding of cell dynamics during thermal treatments.

Photothermal treatment of cancer cells consists in a controlled heating above their physiological temperature (37 ºC) by means of an external light source. Therapeutic effects of such heating arise from the activation of different biological, physical and chemical phenomena that could result in permanent or temporal modifications at the cellular level.[1] The alterations induced in the treated cells strongly depend on the amount of heating, ranging from transient to irreversible damage when temperature is increased from 41 up to 60ºC. [2] Despite the existence of different cell damage types, there is still a big lack of knowledge concerning the exact cellular mechanisms responsible of them. Such knowledge requires the design and performance of photothermal experiments at the single cell level. The simultaneous developing of nanotechnology and bioimaging techniques have made such experiments possible. First results evidenced that a proper interpretation of single cell photothermal treatments needs an accurate monitoring of both intracellular and extracellular temperatures. [3] While intracellular temperature is necessary to explain the damage induced in the cell under treatment, the exact knowledge of the thermal gradient created in its surroundings is fundamental to explain the damage appearing in neighboring cells.[4] The magnitude and extension of thermal gradients in the surrounding of cells and other heating objects in aqueous media have been estimated and postulated in the past, but neither have been experimentally measured.[5]

Thermal sensing at the cellular level should be achieved with minimum perturbation, i.e. in absence of physical contact between cells and sensing units.[4, 6, 7] Among the different approaches proposed for contactless cellular sensing, the use of Luminescent Thermometry (LT) has been found to be especially interesting.[8, 9] LT is based on the use of luminescent probes (Luminescent Thermometers, LThs) which optical properties show a remarkable temperature dependence.[8, 10, 11, 12] In most cases, thermal sensing at cellular level has been achieved after massive incorporation of LThs into the cells. Based on this approach, several groups have managed to get high resolution thermal images of living cells and individual living organisms during photothermal treatments.[6, 12, 13] Nevertheless, such a massive incorporation

could lead to the appearance of undesirable cytotoxic effects.[14] An alternative approach consists in the incorporation into the cellular environment of a single LTh that could be remotely controlled.[15, 16] Optical Trapping (OT) is a versatile and reliable non-contact tool for three-dimensional manipulation of colloidal micro/nano sized objects.[17, 18, 19] OT is based on the forces exerted by a tightly focused laser beam on micro/nanoparticles due to momentum exchange or to the field induced changes in their polarizability. OT of colloidal LThs is, in principle, possible with the additional advantage of simultaneous excitation of their luminescence if the wavelength of the trapping beam is tuned to any absorption band of the LTh. Under this approach, thermal reading at the laser trap position (through particle luminescence) and three dimensional localization of LTh, become possible.[19, 20] Despite the great potential of this approach and its apparent technical simplicity, it still remains an unexplored possibility.

In this work we have demonstrated that thermal scanning at the cellular level is possible by a simple single-beam-single-particle approach. The novelty of this approach is that it involves simultaneous OT and luminescence analysis of a single LTh. This possibility has been demonstrated by using colloidal $NaYF_4:Er^{3+},Yb^{3+}$ particles as sensing units. The choice of such particular crystal particles is motivated by their outstanding ratiometric thermal sensitivity ($>10^{-2}$ $^oC^{-1}$).[10] The potential of OT-assisted contactless thermal sensing for *in vitro* studies has been demonstrated by measuring the thermal gradients created in the surroundings of a single cancer cell subjected to a plasmonic mediated photothermal therapy.

Figure S1(a) in the Supporting Information includes the Scanning Electron Microscopy (SEM) images and size histograms of the different $NaYF_4:Er^{3+},Yb^{3+}$ particles used in this work. Up to four different hexagonal $NaYF_4:Er^{3+},Yb^{3+}$ particles have been investigated, with dimensions (thickness, diameter) of (0.4 µm, 0.8 µm), (0.5 µm, 1.5 µm), (0.7 µm, 2 µm) and (1.6 µm, 3 µm), respectively. All the samples showed a high structural quality (see Figure S1(b)) as well good colloidal stability in distilled water. **Figure 1(a)** shows the experimental setup used for

OT of a single $NaYF_4:Er^{3+},Yb^{3+}$ particle (see Figure 1(b)). A diluted aqueous solution of $NaYF_4:Er^{3+},Yb^{3+}$ particles was introduced in a microchannel, into which a 980 nm laser beam was tightly focused by a single microscope objective. When a $NaYF_4:Er^{3+},Yb^{3+}$ particle is optically trapped, a strong green emission is generated from the trap, as it can be observed in Figure 1(a) as well as in the representative video included in the Supporting Information (see **Video S1**). This green emission, generated by Er^{3+} ions, results from a process known as Energy-Transfer assisted Upconversion (see the schematic energy level diagram of Figure 1(c)) that has been widely used for biosensing and bioimaging.[21, 22, 23] A typical upconversion spectrum in the 500-570 nm spectral range generated by an optically trapped $NaYF_4:Er^{3+},Yb^{3+}$ particle is included in Figure 1(d). As can be observed in Figure 1(d), Er^{3+} ions show two intense bands centered at 530 and 550 nm that correspond to the $^2H_{11/2}\rightarrow{}^4I_{15/2}$ and $^4S_{3/2}\rightarrow{}^4I_{15/2}$ transitions, respectively (see Figure 1(c))[10]. As these emission bands are generated from two thermally coupled excited states, the ratio between their emitted intensities is strongly temperature dependent allowing for accurate thermal sensing.[21, 23] Figure 1(d) shows the luminescence spectra generated by an optically trapped $NaYF_4:Er^{3+},Yb^{3+}$ particle (3 μm in diameter) as obtained when the aqueous dispersion temperature was set to 10 and 36 ºC. As can be observed, a rise in temperature causes an increment in the intensity ratio, $R=I_1/I_2$ ratio, between the 540 and 525 nm bands. This is due to the temperature-induced increase (decrease) of the population of the $^2H_{11/2}$ ($^4S_{3/2}$) excited state.[21] **Figure S2** in the Supporting Information shows the temperature dependence of the intensity ratio *R* as obtained from an optically trapped $NaYF_4:Er^{3+},Yb^{3+}$ (data obtained varying the medium temperature). The observed linear relation between *R* and temperature evidences that the local temperature can be accurately measured from the analysis of the luminescence generated by the optically trapped particle. Thermal sensitivity of LThs, *S*, is typically defined as $S=(dR/dT)\cdot(R)^{-1}$. Linear fit of the included in Figure S2 leads to a thermal sensitivity close to $1.6\cdot10^{-2}\pm0.1\cdot10^{-2}$ $ºC^{-1}$ at 25 ºC. This thermal sensitivity is found to be in good agreements with those previously reported for other Er^{3+},Yb^{3+}

systems.[21] At this point it should be noted that the spectral distribution of the upconversion spectrum generated by individual $NaYF_4:Er^{3+},Yb^{3+}$ particles has been found to slight vary from particle to particle as it is shown in Section S4 of Supporting Information.

The possibility of 3D manipulation and scanning of a single $NaYF_4:Er^{3+},Yb^{3+}$ particle by OT in a cellular medium would depend on the magnitude of the optical forces exerted on it that should be overcome in order to overcome drag forces created by fluid viscosity. The magnitude of OT forces acting on the different $NaYF_4:Er^{3+},Yb^{3+}$ particles was measured by the hydrodynamic drag method, as explained in detail in Section S3 of the Supporting Information.[18, 24] A representative force *vs* power plot is included in **Figure 2(a),** from which the trapping constant (K_{trap}, OT force divided by laser power) can be calculated. K_{trap} was found to be strongly dependent on both the Numerical Aperture (NA) of the microscope objective and the $NaYF_4:Er^{3+},Yb^{3+}$ particle size as it was expected.[16] This fact is evidenced in Figure 2(b-c). Figure 2(b) shows the dependence of K_{trap} on the $NaYF_4:Er^{3+},Yb^{3+}$ particle size as obtained for a microscope objective of NA=0.8 that produces a laser spot diameter close to 1.4 μm. These were found to be the optimum trapping conditions for the 2 μm diameter $NaYF_4:Er^{3+},Yb^{3+}$ particles. This fact suggests that the optical force is maximized when the $NaYF_4:Er^{3+},Yb^{3+}$ particle diameter slightly exceeds the laser spot diameter. This suggestion has been corroborated in Figure 2(c), in which we have systematically investigated the OT force acting on 3 μm sized $NaYF_4:Er^{3+},Yb^{3+}$ particles as a function of the NA of the focusing objective. OT force is maximum when the NA is set to 0.55, which leads to a laser spot diameter of 2.2 μm (slightly smaller than particle size). From Figure 2(c) it is clear that an adequate choice of focusing optics could lead to trapping constants as large as 60 fN/mW, allowing for their stable scanning in the surroundings of cells by using moderate laser trapping powers. In this sense we have to note that, as discussed in Section S5 of Supporting Information, upconversion from single particles can be detected by using 980 nm laser powers as low a 1 mW ($0.3 \cdot 10^5$ W/cm^2 power density). Nevertheless, the laser power used during the radial thermal scans was set to

be 13 mW ($3.6 \cdot 10^5$ W/cm^2 power density) as it ensures thermal resolutions of 1ºC while keeping the thermal loading induced by trapping ratiation close to 1ºC (see Section S5 in the Supporting Information).[25]

Once simultaneous OT and thermal sensing from a single $NaYF_4:Er^{3+},Yb^{3+}$ particle had been demonstrated, we combined them to elucidate the magnitude and spatial extension of the thermal gradient created in the surroundings of a cancer cell subjected to a plasmonic based photothermal treatment. For such a purpose, we designed the experimental approach schematically represented in **Figure 3(a)** that implies the scanning of an optically trapped $NaYF_4:Er^{3+},Yb^{3+}$ particle in the surroundings of a HeLa cell. Cells were previously incubated with 15x45 nm Gold Nanorods (GNRs). These GNRs have a surface plasmon resonance wavelength peak at 808 nm and a heating efficiency close to unity.[10, 26] Efficient intracellular incorporation of GNRs was verified by multiphoton fluorescence microscopy (see **Figure 4(a)** and **Figure S3**). The incorporation of GNRs allowed for intracellular heating by using an 800 nm laser beam that was focused into the cell by means of a single microscope objective. For thermal measurements in the surroundings of the treated cell, $NaYF_4:Er^{3+},Yb^{3+}$ particles were added to the culture medium. A 980 nm laser beam was used for OT and scanning of a single $NaYF_4:Er^{3+},Yb^{3+}$ particle. OT and particle scanning in the surroundings of a cell should overcome several difficulties that are discussed in detail in Section S6 of Supporting Information. The extension and magnitude of thermal gradients in the surroundings of individual cells was investigated by performing different "horizontal" thermal scans at different particle-to-substrate distances. As explained the Supporting information, the performance of horizontal scans minimizes the possible influence of particle-to-substrate interaction in the output thermal reading. Figure 3(b) shows an $NaYF_4:Er^{3+},Yb^{3+}$ particle (3 μm in diameter, indicated by a green circle) that has been optically manipulated in the proximity of a HeLa cancer cell incubated with GNRs. The location of the 800 nm heating laser spot inside the HeLa cancer cell has been schematically indicated by a red dashed circle. The dashed arrow indicates

the horizontal scan pathway. The temperature increment (in respect to medium temperature, T_{med} = 27 ºC) sensed by the $NaYF_4:Er^{3+},Yb^{3+}$ particle at different horizontal (x) distances from the cell as obtained at different z heights are included in Figure 3(c), where dots correspond to the experimental data and the lines are a guide for the eyes (details about temperature and spatial uncertainties can be found in Section S5 of Supporting Information). Figure 3(c) also includes (bottom graph) the "control" thermal scan obtained when the 800 nm laser beam was switched off, revealing the 800 nm laser radiation as the unique heating source. Figure 4(b) shows the magnitude of the extra-cellular heating as a function of the 800 nm laser power as obtained for control and GNRs incubated cells. It is found that, for cells containing GNRs, the maximum extracellular temperature increases linearly with laser power as it was expected. In absence of internalized GNRs (control experiment), no heating was observed. This reveals GNRs as the unique light-to-heat conversion particles.

From the thermal scans included in Figure 3(c), it is clear that plasmonic-mediated heating is not restricted to the intracellular volume. On contrary, thermal gradients extend distances larger than 10 microns. The existence of such thermal gradients makes real single-cell photo thermal treatment not feasible since not only the treated cell but also all cells in its surroundings will be heated. The extension of the thermal gradient (λ_T) is here defined as the distance at which temperature has been reduced down to 0.5 times the maximum temperature (achieved at the begining of the scan). From data included in Figure 3(c) we have estimated $\lambda_T \approx 6$ μm that is close to the effective radius of the 800 nm laser focal volume. According to the discussion included in Section S7 of Supporting Information, this suggest that the treated cell is acting as a point heating source. Note that the anslysis of the horizontal scans obtained at different heigths also evidences the existence of a vertical thermal gradient with an extension of few microns (when the z coordinate is increased from 5 up to 15 μm the magnitude of extarcellular heating is reduced by almost 80%).

As it is explained in Section S7, the extension of thermal gradients is expected to be strongly dependent on the geometry of the heating source. For instance, the extension of thermal gradients created by a cylindrical heating source in a microfluidic chamber is expected to be of the order of the chamber height. In order to double check the validity of our approach for the determination of thermal gradients we designed an additional control experiment that is schematically represented in **Figure S9(a)**. In this case, the thermal gradient was created by focusing a 1480 nm laser beam (partially absorbed by water see **Figure S10**) into a 100 μm height microchannel. The spatial extension of the thermal pattern created by water absorption has been measured by scanning an optically trapped $NaYF_4:Er^{3+},Yb^{3+}$ particle in an orthogonal direction to the 1480 nm laser beam path. The experimentally measured temperature profile is shown in Figure S9(a). The highest temperature (that is proportional to the 1480 nm laser power as shown in Figure S9(b)) was obtained at the focus of the 1480 nm laser beam. From the temperature profile included in Figure S9, a thermal gradient extension of 100 μm was obtained, being this comparable to the chamber height. This well agrees with theoretical predictions for heating source with cylindrical symmetry, as it is explained in detail in Section S7. Such excellent agreement confirms the reliability of our approach for accurate determination of thermal gradients at the microscale.

3. Conclusion

In summary, this work demonstrates how thermal sensing in the surroundings of a single cancer cell with a micrometric spatial resolution and a sub-degree thermal accuracy is possible by remote (contactless) scanning of a single optically driven/excited luminescent thermometer. This has been demonstrated by scanning an infrared optically trapped $NaYF_4:Er^{3+},Yb^{3+}$ upconverting particle. Partial absorption of the 980 nm trapping laser beam allowed for simultaneous three-dimensional manipulation and fluorescence ratiometric thermal sensing by using a simple experimental design. This novel approach has been used to elucidate the magnitude and spatial extension of the thermal gradient appearing in the surroundings of a

plasmonic mediated photothermally treated cancer cell. Thermal gradient has been found to extend over ten microns affecting surrounding cells and avoiding single cell treatment.

Results included in this work constitute the first step towards the achievement of minimally invasive, contactless, high-sensitivity three-dimensional thermal imaging of microsized systems. The results here reported constitute the proof of concept and a wide working field is now open for the optimization of the thermal sensing particle and three-dimensional optical trapping systems.

Experimental Section

$NaYF_4:Er^{3+},Yb^{3+}$ particles synthesis: The $NaYF_4:Er^{3+},Yb^{3+}$ particles were synthesized by the hydrothermal method. More details about the synthesis process can be found in the Supporting Information.

Optical trapping: $NaYF_4:Er^{3+},Yb^{3+}$ particles were optically trapped in a homemade single-beam optical tweezer setup. Laser radiation coming from a 980 nm single-mode fiber-coupled laser diode was used for both trapping and exciting the $NaYF_4:Er^{3+},Yb^{3+}$ particle. The hydrodynamic drag method was used to calculate the optical forces exerted over the different particles. Details about force calculation procedure and the optical system used for optical trapping experiments can be found in the Supporting Information.

Thermal sensing: Luminescence spectra of optically trapped $NaYF_4:Er^{3+},Yb^{3+}$ particles was spectrally analyzed by a high sensitivity Si CCD camera (Synapse, Horiba) attached to a monochromator (iH320, Horiba) all it optically coupled to the single-beam optical tweezers setup. Calibration curves were acquired by varying the temperature of the aqueous solution contained the optically trapped $NaYF_4:Er^{3+},Yb^{3+}$ particle while performing simultaneous spectrum acquisition and analysis. Thermal resolution has been estimated from the signal/noise ratio of upconverted spectra to be ±1ºC. More detail can be found in the Supporting Information.

Cell preparation: Single cell plasmonic mediated photothermal treatments were performed on HeLa cancer cells after incubation with Gold Nanorods with surface plasmon resonance at 808 nm. An 800 nm fiber coupled laser diode was focused into a HeLa cell promoting plasmonic mediated heating. Heating laser power was set to 15 mW. Further details about the cell preparation procedure can be found in the Supporting Information.

Supporting Information

Supporting Information is available from the Wiley Online Library or from the author.

Acknowledgements

This work was supported by the Spanish Ministerio de Educación y Ciencia (MAT2013–47395-C4–1-R) and by Banco Santander for "Proyectos de Cooperación Interuniversitaria" (2015/ASIA/06). P.H.G thanks the Spanish Ministerio de Economía y Competitividad (MINECO) for the Juan de la Cierva program. P.R.S thanks the Spanish Ministerio de Economía y Competitividad (MINECO) for the "Promoción del talento y su Empleabilidad en I+D+i" statal program.

Received: ((will be filled in by the editorial staff))
Revised: ((will be filled in by the editorial staff))
Published online: ((will be filled in by the editorial staff))

REFERENCES

[1] J. Van der Zee, Annals of oncology 2002, 13, 1173; P. Wust, B. Hildebrandt, G. Sreenivasa, B. Rau, J. Gellermann, H. Riess, R. Felix, P. M. Schlag, Lancet Oncol 2002, 3, 487.
[2] A. Chicheł, J. Skowronek, M. Kubaszewska, M. Kanikowski, Reports of Practical Oncology & Radiotherapy 2007, 12, 267; M. Johannsen, U. Gneveckow, L. Eckelt, A. Feussner, N. Waldofner, R. Scholz, S. Deger, P. Wust, S. A. Loening, A. Jordan, Int J Hyperthermia 2005, 21, 637; J. Mendecki, E. Friedenthal, C. Botstein, R. Paglione, F. Sterzer, International journal of radiation oncology, biology, physics 1980, 6, 1583; E. Day, P. A. Thompson, L. Zhang, N. A. Lewinski, N. Ahmed, Journal of Neuro-Oncology 2011, 104, 55; W. Zhang, Z. Guo, D. Huang, Z. Liu, X. Guo, H. Zhong, Biomaterials 2011, 32, 8555; C. J. Diederich, Int. J. Hyperthermia 2005, 21, 745; R. W. Habash, R. Bansal, D. Krewski, H. T. Alhafid, Crit Rev Biomed Eng 2007, 35, 37; S. V. Torti, F. Byrne, O. Whelan, N. Levi, B. Ucer, M. Schmid, F. M. Torti, S. Akman, J. Liu, P. M. Ajayan, O. Nalamasu, D. L. Carroll, Int J Nanomedicine 2007, 2, 707; B. J. Wood, Z. Neeman, A. Kam, in *Tumor Ablation*, Springer, 2005, 285.
[3] H. Y. Nam, S. M. Kwon, H. Chung, S.-Y. Lee, S.-H. Kwon, H. Jeon, Y. Kim, J. H. Park, J. Kim, S. Her, Y.-K. Oh, I. C. Kwon, K. Kim, S. Y. Jeong, J. Controlled Release 2009, 135, 259.
[4] L. M. Maestro, P. Haro-Gonzalez, M. C. Iglesias-de la Cruz, F. Sanz-Rodriguez, A. Juarranz, J. G. Sole, D. Jaque, Nanomedicine 2013, 8, 379.
[5] N. Manuchehrabadi, L. Zhu, International Journal of Hyperthermia 2014, 30, 349; R. Singh, K. Das, S. C. Mishra, J. Therm. Biol. 2014, 44, 55; A. AlAmiri, K. Khanafer, K. Vafai, Numerical Heat Transfer Part a-Applications 2014, 66, 1; G. Baffou, R. Quidant, C. Girard, Physical Review B 2010, 82, 165424.
[6] F. Wang, D. Banerjee, Y. Liu, X. Chen, X. Liu, Analyst 2010, 135, 1839; D. K. Chatterjee, M. K. Gnanasammandhan, Y. Zhang, Small 2010, 6, 2781.
[7] D. Jaque, B. del Rosal, E. Martin Rodriguez, L. Martinez Maestro, P. Haro-Gonzalez, J. Garcia Sole, Nanomedicine 2014, 9, 1047.
[8] D. Jaque, F. Vetrone, Nanoscale 2012, 4, 4301; C. D. S. Brites, P. P. Lima, N. J. O. Silva, A. Millan, V. S. Amaral, F. Palacio, L. D. Carlos, New Journal of Chemistry 2011, 35, 1177.
[9] C. D. S. Brites, P. P. Lima, N. J. O. Silva, A. Millan, V. S. Amaral, F. Palacio, L. D. Carlos, Nanoscale 2012, 4, 4799.
[10] F. Vetrone, R. Naccache, A. Zamarron, A. J. de la Fuente, F. Sanz-Rodriguez, L. M. Maestro, E. M. Rodriguez, D. Jaque, J. G. Sole, J. A. Capobianco, Acs Nano 2010, 4, 3254.
[11] M. A. Bennet, P. R. Richardson, J. Arlt, A. McCarthy, G. S. Buller, A. C. Jones, Lab on a chip 2011, 11, 3821; U. Rocha, C. Jacinto, W. F. Silva, I. Guedes, A. Benayas, L. M. Maestro, M. A. Elias, E. Bovero, F. van Veggel, J. A. G. Sole, D. Jaque, ACS Nano 2013, 7, 1188; C. Gota, K. Okabe, T. Funatsu, Y. Harada, S. Uchiyama, Journal of the American Chemical Society 2009, 131, 2766; L. Shang, F. Stockmar, N. Azadfar, G. U. Nienhaus, Angewandte Chemie International Edition 2013, 52, 11154.
[12] J. S. Donner, S. A. Thompson, M. P. Kreuzer, G. Baffou, R. Quidant, Nano Letters 2012, 12, 2107; A. P. Sudarsan, V. M. Ugaz, Proceedings of the National Academy of Sciences 2006, 103, 7228.
[13] G. Baffou, H. Rigneault, D. Marguet, L. Jullien, Nat Meth 2014, 11, 899; J.-M. Yang, H. Yang, L. Lin, ACS Nano 2011, 5, 5067; J. S. Donner, S. A. Thompson, C. Alonso-Ortega, J. Morales, L. G. Rico, S. I. C. O. Santos, R. Quidant, ACS Nano 2013, 7, 8666.
[14] K. Okabe, N. Inada, C. Gota, Y. Harada, T. Funatsu, S. Uchiyama, Nat Commun 2012, 3, 705.
[15] L. Aigouy, L. Lalouat, M. Mortier, P. Löw, C. Bergaud, Review of Scientific Instruments 2011, 82; E. Hemmer, N. Venkatachalam, H. Hyodo, A. Hattori, Y. Ebina, H.

Kishimoto, K. Soga, Nanoscale 2013, 5, 11339; L. Aigouy, A. Cazé, P. Gredin, M. Mortier, R. Carminati, Physical Review Letters 2014, 113, 076101.
[16] L. Aigouy, G. Tessier, M. Mortier, B. Charlot, Applied Physics Letters 2005, 87, 1.
[17] M. Dienerowitz, M. Mazilu, K. Dholakia, Journal of Nanophotonics 2008, 2, 021875; H. Zhang, K. K. Liu, Journal of the Royal Society Interface 2008, 5, 671; A. Ashkin, Proceedings of the National Academy of Sciences of the United States of America 1997, 94, 4853; A. Ashkin, J. M. Dziedzic, T. Yamane, Nature 1987, 330, 769.
[18] W. H. Wright, G. J. Sonek, M. W. Berns, Appl. Opt. 1994, 33, 1735.
[19] P. M. Bendix, L. Jauffred, K. Norregaard, L. B. Oddershede, Ieee Journal of Selected Topics in Quantum Electronics 2014, 20.
[20] P. Haro-Gonzalez, W. T. Ramsay, L. M. Maestro, B. del Rosal, K. Santacruz-Gomez, M. D. Iglesias-de la Cruz, F. Sanz-Rodriguez, J. Y. Chooi, P. R. Sevilla, M. Bettinelli, D. Choudhury, A. K. Kar, J. G. Sole, D. Jaque, L. Paterson, Small 2013, 9, 2162; F. M. Mor, A. Sienkiewicz, L. Forró, S. Jeney, ACS Photonics 2014, 1, 1251.
[21] P. Haro-Gonzalez, B. del Rosal, L. M. Maestro, E. Martin Rodriguez, R. Naccache, J. A. Capobianco, K. Dholakia, J. G. Sole, D. Jaque, Nanoscale 2013, 5, 12192.
[22] T. V. Gavrilović, D. J. Jovanović, V. Lojpur, M. D. Dramićanin, Sci. Rep. 2014, 4; F. Auzel, Journal of Luminescence 1990, 45, 341; N. Phuong-Diem, S. J. Son, J. Min, Journal of Nanoscience and Nanotechnology 2014, 14, 157; S. Zeng, Z. Yi, W. Lu, C. Qian, H. Wang, L. Rao, T. Zeng, H. Liu, H. Liu, B. Fei, J. Hao, Adv. Funct. Mater. 2014, 24, 4196; Y. I. Park, H. M. Kim, J. H. Kim, K. C. Moon, B. Yoo, K. T. Lee, N. Lee, Y. Choi, W. Park, D. Ling, Adv. Mater. 2012, 24, 5755; S. H. Nam, Y. M. Bae, Y. I. Park, J. H. Kim, H. M. Kim, J. S. Choi, K. T. Lee, T. Hyeon, Y. D. Suh, Angewandte Chemie 2011, 123, 6217.
[23] F. Auzel, Chem Rev 2004, 104, 139.
[24] K. Dholakia, P. Reece, M. Gu, Chemical Society Reviews 2008, 37, 42.
[25] P. Haro-González, W. T. Ramsay, L. M. Maestro, B. del Rosal, K. Santacruz-Gomez, M. del Carmen Iglesias-de la Cruz, F. Sanz-Rodríguez, J. Y. Chooi, P. R. Sevilla, M. Bettinelli, D. Choudhury, A. K. Kar, J. G. Solé, D. Jaque, L. Paterson, Small 2013, 9, 2162.
[26] D. Jaque, L. Martinez Maestro, B. del Rosal, P. Haro-Gonzalez, A. Benayas, J. L. Plaza, E. Martin Rodriguez, J. Garcia Sole, Nanoscale 2014, 6, 9494; L. M. Maestro, P. Haro-Gonzalez, A. Sanchez-Iglesias, L. M. Liz-Marzan, J. Garcia Sole, D. Jaque, Langmuir 2014, 30, 1650.

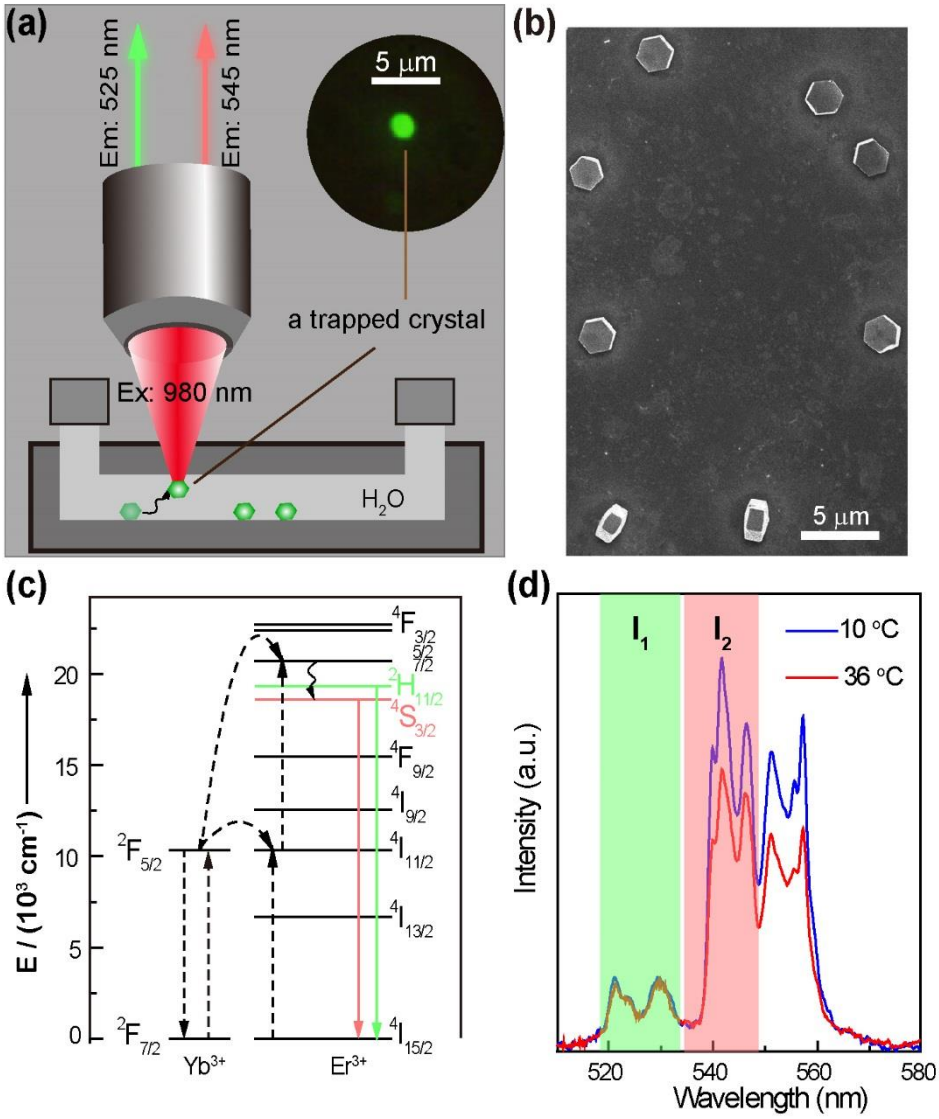

Figure 1. (a) Schematic representation of the experimental setup used in this work for thermal sensing by an optically trapped $NaYF_4:Er^{3+},Yb^{3+}$ particle (5/0.5 mol%). **(b)** A typical scanning electron microscopic image of $NaYF_4:Er^{3+},Yb^{3+}$ particle, showing a clear hexagonal morphology. **(c)** Simplified energy level diagram showing the temperature sensitive energy levels, $^2H_{11/2}$ and $^4S_{3/2}$, (in highlighted colors) and the corresponding energy transition processes. **(d)** Emission spectra obtained from a single optically trapped $NaYF_4:Er^{3+},Yb^{3+}$ particles at two different temperatures. The intensity ratio I_1/I_2 is highly temperature-sensitive.

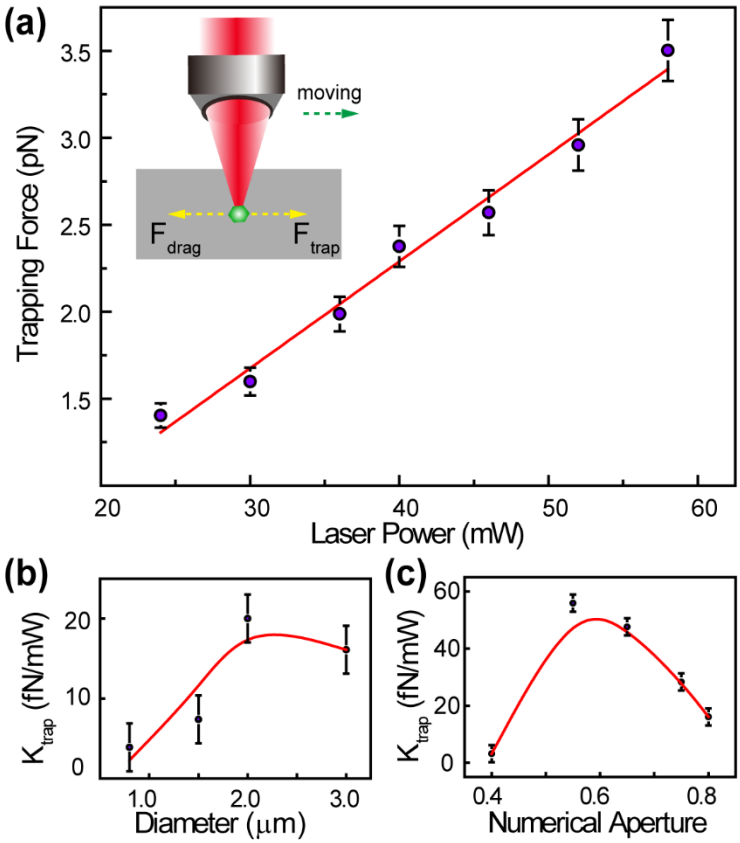

Figure 2. (a) Optical trapping force on a $NaYF_4:Er^{3+},Yb^{3+}$ particles as a function of the 980 nm laser power. Numerical aperture of the focusing objective was 0.55. Inset shows a diagram indicating how the optical force is measured in this work. **(b)** Optical trapping constant (K_{trap}) as a function of the diameter of the particle. Data were obtained using a NA = 0.8 focusing objective. Dots correspond to the experimental data and the solid line is a guide for the eyes. **(c)** Optical trapping constant (K_{trap}) as obtained for a 3 μm in diameter $NaYF_4:Er^{3+},Yb^{3+}$ particles as a function of the numerical aperture of the focusing objective. Dots are experimental data and the solid line is a guide for the eyes.

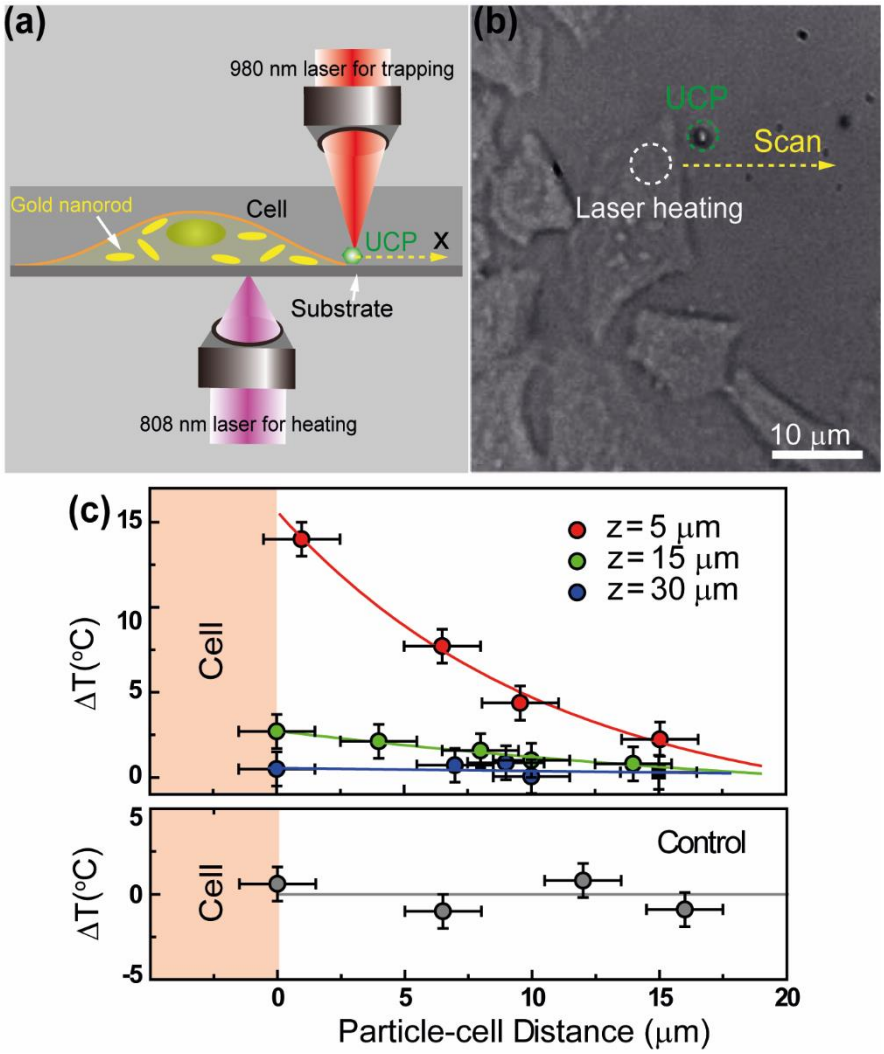

Figure 3. **(a)** Schematic representation of the experimental setup used for thermal scanning in the surroundings of a HeLa cell subjected to a plasmonic mediated photothermal treatment. The thermal scan direction is indicated with a yellow arrow. **(b)** The optical transmission image of the HeLa cancer cells after incubation with GNRs. The dashed circle indicates the position of the (heating) 800 nm laser spot. The presence of the $NaYF_4:Er^{3+},Yb^{3+}$ particle used for thermal measurements is also indicated by a green dashed circle. **(c)** Upper part. Temperature decay measured from cell surface for three heights (distances from substrate). Dots are experimental data, and lines are a guide for the eyes. Down part. Control thermal scan performed in absence of the 800 nm heating laser.

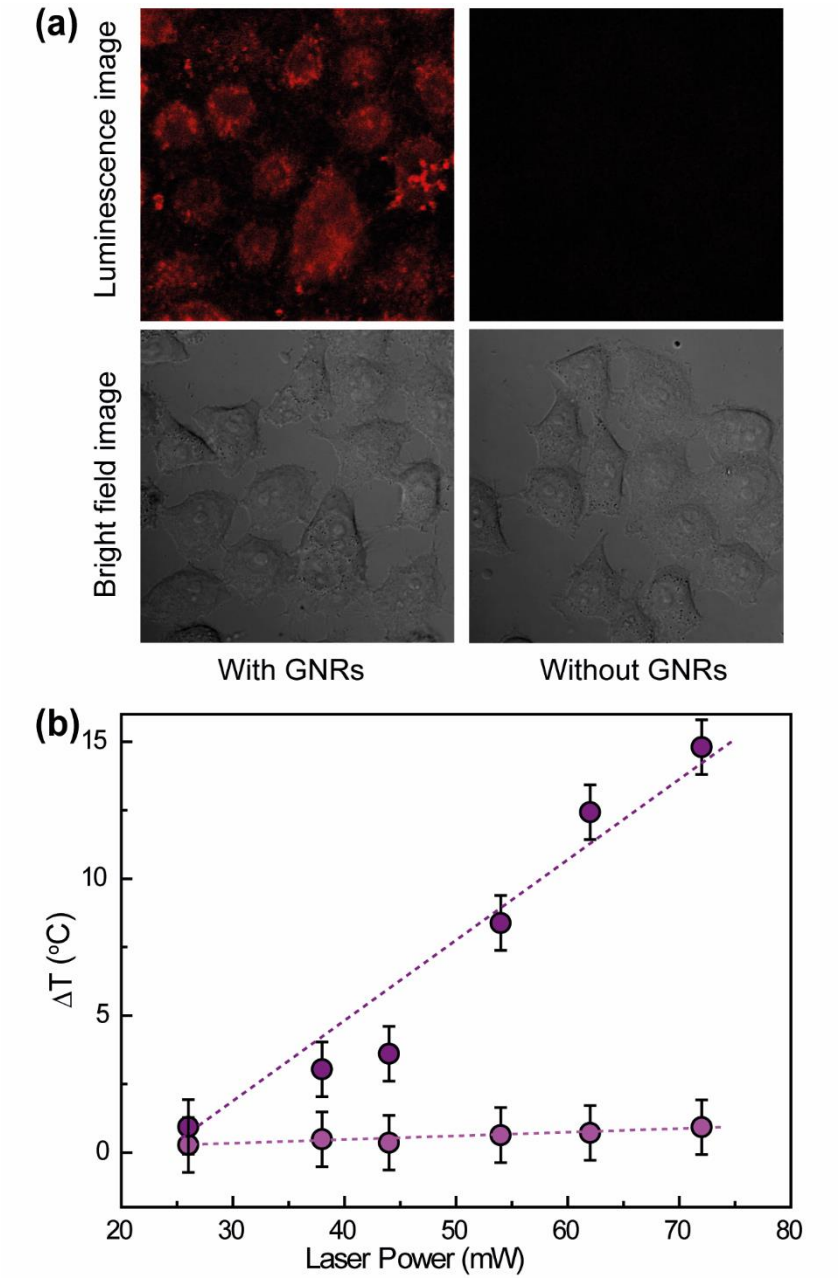

Figure 4. (a). Luminescence (upper part) and optical (lower part) images of the used HeLa cells incubated with (left) and without (right) GNRs. A clear difference in the luminescence denotes the presence of GNRs inside the cells. **(b).** Maximum temperature increment induced in the surrounding of a cell incubated with (purple data) and without (pink data) as a function of the laser power of the 800 nm laser heating.

The table of contents entry.

3D optical manipulation of a thermal sensing upconverting particle allows for the determination of the extension of the thermal gradient created in the surroundings of a plasmonic mediated photothermal treated HeLa cancer cell.

ToC figure